JOURNAL OF MATERIALS SCIENCE 14 (1979) 2091–2102

Strength and fracture properties of asbestos-cement mortar composites

Y. W. MAI
Department of Mechanical Engineering, The University of Sydney, Sydney, New South Wales, Australia

The strength and fracture properties of random asbestos fibre-reinforced cement mortar composites are reported in this paper. The fibre content varies between 5% and 20% by weight. Both the ultimate tensile strength (σ_t) and the modulus of rupture (σ_b) increase with increasing fibre-volume fraction. These results are shown to agree satisfactorily with the law of mixtures modified for randomly oriented short fibre-reinforced composites. The critical stress intensity factor (K_c) and the specific work of fracture (R) have been determined using three-point bend edge-notched beams and grooved double-cantilever-beam (DCB) specimens. There is generally good agreement between these two physical quantities estimated from the two testpiece geometries. It is shown that the fibre pull-out mechanism is dominant in the fracture of asbestos cements and that the specific work of fracture can be reasonably well predicted by considering the energies absorbed in both the pull-out and the fibre/matrix interfacial debonding processes.

1. Introduction

Asbestos cement is a composite material made up of short asbestos fibres randomly dispersed in a cement mortar matrix. It is widely used in the building industry for making fire-proofing and insulating materials, sewer pipes, corrugated and flat sheets for roof covering and wall lining. In such applications it is necessary that the asbestos cement products possess an acceptable bending strength and resistance to crack propagation.

With the continuing demand for asbestos fibres it is apparent that prices will eventually become uneconomical to justify their use for reinforcement of cements. Thus there is a need to search for a suitable substitute fibre for cement reinforcement. The use of glass fibres, carbon fibres and organic polymeric filaments such as polypropylene and nylon as suitable substitute fibres has been studied by Majumdar and co-workers [1–3]. It is found that to obtain both good impact resistance and high bending strength a mixture of organic and inorganic fibres is needed in the cement [1]. Recently, Walton and Majumdar [4] have demonstrated that the new polyamide fibre, Kevlar, is probably the most promising substitute fibre to give efficient reinforcement for cementitious matrices. Good composite strength (similar to asbestos cements) and high impact toughness (approximately ten-fold increase) have been obtained in these Kevlar-cement composites [4].

The basic considerations for a good replacement fibre are that it shall produce a resultant composite which possesses strength, crack resistance and other mechanical and physical properties similar to asbestos cements. This choice cannot be properly made until we have a complete understanding of the independent properties of the cement mortar matrix, the asbestos fibres, the fibre/matrix interface and the reinforcing mechanisms for the asbestos cement composites. Aveston [5] and Martin and Phillips [6] have considerably advanced our knowledge of the physical texture and mechanical strength of the asbestos fibres. Walsh *et al.* [7] and Birchall *et al* [8] have provided detailed explanations for the brittle strength of cements. However, in

0022–2461/79/092091–12 $03.20/0

relation to composites, apart from the early preliminary study of Allen [9], it appears that there has not been any systematic work on the strength and fracture properties of asbestos cements published in the open literature. Information on the interfacial properties including the bonding nature of asbestos fibres to cement mortar matrices and on the source of fracture toughness in such asbestos cement composites is particularly lacking at present. This paper only deals with the latter problem to elucidate the fracture mechanisms of asbestos cements and is not concerned with the fibre/cement matrix interface problem which is the subject of a future investigation. It will be shown (in Section 4.2) that the fibre pull-out process constitutes the major contribution to the total fracture resistance of asbestos cements. The effects of asbestos fibre-volume fraction on the tensile strength, modulus of rupture and specific work of fracture have been investigated in this paper.

2. Theoretical considerations

2.1. Strength of asbestos cement composites

The law of mixtures for aligned continuous fibrous composites may be modified to predict the strength of asbestos cements. It will be assumed that at failure the asbestos fibres are not broken but are pulled out of the cement matrix.* Thus the average tensile stress in the fibre (σ_f) is given by

$$\sigma_f = 2\tau(l/d) \quad (1)$$

where τ is the fibre–matrix interfacial bond strength, l and d are the length and diameter of the asbestos fibre. With random orientation of the short fibres, only those which are parallel or nearly parallel to the loading direction can produce efficient reinforcement. For fibres which are less favourably oriented full reinforcement will not be achieved and an efficiency factor must be applied. By assuming uniform distribution of fibres in the matrix, Romualdi and Mandel [10] have shown that the effective fibre-volume fraction is 41% of the nominal volume fraction if the fibres can be orientated in any direction with equal probability. It is therefore possible to rewrite the ultimate tensile strength (σ_t) equation for the asbestos cement composite as:

$$\sigma_t = \sigma_m v_m + 0.41\,\sigma_f v_f, \quad (2)$$

where σ_m is the tensile strength of the unreinforced cement mortar matrix and v_m, v_f are the volume fractions of the matrix and the asbestos fibres, respectively. This is reduced to

$$\sigma_t = \sigma_m v_m + 0.82\tau v_f(l/d) \quad (3)$$

using Equation 1 for σ_f. Equation 3 may be extended to predict the modulus of rupture (σ_b) of asbestos cements since in general we have $\sigma_b = \alpha\sigma_t$ and $\sigma_{mb} = \beta\sigma_m$, where α, β are constants which can be determined from experiments and σ_{mb} is the modulus of rupture of the cement mortar matrix in bending. Thus,

$$\sigma_b = \left(\frac{\alpha}{\beta}\right)\sigma_{mb} v_m + 0.82(\alpha\tau) v_f(l/d). \quad (4)$$

Equations 3 and 4 were first given by Swamy and Mangat [11] for concrete reinforced with randomly distributed short steel fibres.

2.2. Critical stress intensity factor and specific work of fracture of asbestos cement composites

Linear elastic fracture mechanics concepts were first applied by Kaplan [12] to concrete and subsequently extended to cement paste, mortar and random short fibre-reinforced concrete by others [13–16]. Fracture parameters such as the critical stress intensity factor (K_c) and the critical strain energy release rate (G_c) have been studied by a number of different methods. Although linear elastic fracture mechanics is strictly speaking inapplicable for these materials which are microscopically heterogenous and anisotropic, the success of using toughness parameters as fracture criteria has been clearly demonstrated by experimental results which indicate that $EG_c \simeq K_c^2$ where G_c and K_c are measured independently. Of course, for this relationship to hold, the pseudo plastic zone size and any inelastic effects at the crack tip must be small. It should be noted that both K_c and G_c correspond to fracture initiation values and where no slow crack growth occurs they become fracture instability values. It is expected that this linear elastic fracture mechanics approach will be applicable to asbestos cements. Mindess *et al.* [17] recently have suggested the use of the J-integral [18] to give a more realistic fracture parameter for fibre-reinforced concrete. J_c, which is the critical J value at crack initiation can be experimentally determined using one deep

* This assumption is justified since microscopic examination of fracture surfaces show little sign of fibre breakage.

edge-notched and one unnotched specimen subjected to bending [17]. It will be shown that for the asbestos cements studied in this work the load–deflection curve is linear to the point of crack propagation. Thus, for this linear elastic situation,

$$J_c = G_c \simeq K_c^2/E, \quad (5)$$

so that the J-integral approach and the K_c or G_c analysis are equivalent.

The work of fracture method [19] has also been used to measure the specific fracture resistance* (R) of fibre-reinforced composites using three-point bend notched specimens. R is given by (see Fig. 1)

$$R = \frac{U}{B(W-a)} \quad (6)$$

where U is the integrated area under the load–deflection curve which includes both the crack initiation (U_i) and crack propagation (U_p) energies, B is the specimen thickness, W is the width and a is the notch depth. R is usually not a constant (especially for strain-rate sensitive materials) and decreases with increasing a/W. To determine valid values of R it is necessary that crack propagation is stable and continuous, otherwise if unstable cracking occurs, the specific work of fracture estimated from the saw-tooth load–deformation curve is an upper bound value. It is also possible to define a crack-initiation resistance parameter (R_i) by

$$R_i = \frac{U_i}{B(W-a)}. \quad (7)$$

This initiation value assumes that all U_i is released for crack propagation over the ligament area $B(W-a)$ and is thus identical to J_c, G_c and K_c^2/E as described previously. Unlike R, R_i is independent of a/W for fibrous composite materials [20].

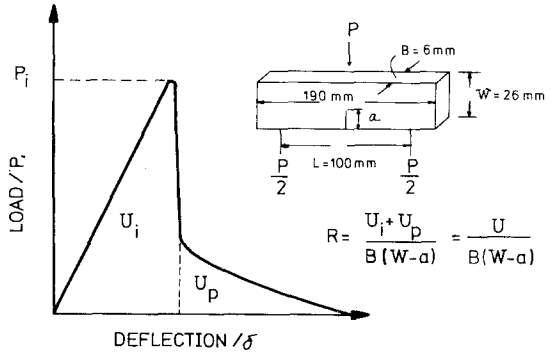

Figure 1 Schematic diagram for R determination by the work of fracture method.

The work of fracture method [19] suffers two limitations in its usefulness for the determination of R. Firstly cracking is normally unstable unless a/W is relatively large. The a/W ratio at which stable cracking commences depends on the asbestos fibre volume fraction. Secondly even if cracking is stable, only one R value is obtained per specimen. Gurney and Hunt [21] have developed a quasi-static crack propagation technique which is suitable for the determination of specific work of fracture (R) of asbestos cements in specimens where crack propagation is stable and where there is no irreversible deformation at regions remote from the crack tip. An appropriate specimen such as the double-cantilever-beam (DCB) configuration may be used conveniently with the Gurney method to yield several R measurements per test-piece. For asbestos cements R is expected to increase with crack length (in DCB specimens) since more and more fibres that bridge the crack opening are being pulled out as the crack advances. Patterson and Chan [22] have demonstrated the general validity of the Gurney approach for R measurements in glass fibre-reinforced cements.

2.3. Source of fracture toughness of asbestos cements

A generalized theory has been proposed by Marston *et al.* [23] where the specific fracture resistance (R) is given by the sum of the separate toughnesses resulting from fibre pull-out (R_{po}), redistribution of stresses (R_{re}) and fracture of surfaces (R_s). For the asbestos cements studied here the average fibre length (l) is less than the critical transfer length (l_c) (see Section 4.1) and it seems, therefore, appropriate to neglect R_{re} as a component contribution to the specific work of fracture (R). Thus

$$R = R_{po} + R_s \quad (8)$$

where for $l < l_c$, so that fracture of fibres does not occur,

$$R_{po} = \frac{0.41\, v_f l^2 \tau}{6d} \quad (9)$$

and

$$R_s = v_m R_m + (0.41 v_f)\frac{4\bar{l}R_{if}}{d}. \quad (10)$$

*Usually the symbol (2γ) is used for R by other research workers. It measures the average fracture energy per unit crack area over the entire fracture process.

$\bar{l}(\simeq l/4)$ is the average pull-out length of the asbestos fibres and R_m, R_{if} are the fracture energies of the cement mortar matrix, and fibre–matrix interface, respectively. Since Equations 9 and 10 are originally derived for composites with aligned fibres and since the effective volume fraction of reinforcement is less than the nominal v_f in random fibre composites, an effeciency factor of 0.41 (the same as that used in Equation 2) is applied to these toughness expressions. Harris *et al.* [14] have adopted a similar correction procedure when analysing the fracture toughness of randomly distributed short steel fibre-reinforced concrete. They have, however, used an experimentally determined value of 0.55 instead of 0.41 because the fibre distribution is not fully random in three dimensions in their material. In the absence of independent data for R_{if}, an upper bound is given by $R_{if} \simeq R_m$ [23] so that Equation 10 is simplified to

$$R_s \simeq 0.41 v_f \frac{l R_m}{d} + v_m R_m. \quad (11)$$

The specific work of fracture (R) is thus given by

$$R = \frac{0.41 v_f l^2 \tau}{6d} + \left[v_m + 0.41 \frac{v_f l}{d} \right] R_m. \quad (12)$$

3. Experimental work

3.1. Material

The asbestos fibre-reinforced cement mortar composites with fibre mass fractions of 5% to 20% were supplied by James Hardie & Coy Pty Ltd. The asbestos was initially fiberized (i.e. split down to fine fibres) by four passes through a laboratory mill which gave the properties shown in Table I before mixing with the silica-cement slurry. Table II gives the composition and the calculated fibre volume fractions of the four formulations of asbestos cements studied in this work. The castings were made in a vacuum filter box approximately 190 mm square.* After curing for 24 h at 100% r.h. they were autoclaved at 0.86 MPa for 8 h. Specimens for strength and fracture tests were then cut on a diamond saw to specified dimensions. For the fracture toughness specimens the last 3 to 4 mm of the required crack length was cut by a blade 0.15 mm thick.

TABLE I Characterization of asbestos fibres

(1) *Bauer–McNett classification*

Material retained on sieve (%)	Test 1	Test 2
4 mesh	32.8	35.0
14 mesh	20.4	17.0
35 mesh	15.4	13.6
200 mesh	12.2	11.6
Through 200 mesh (by difference)	19.2	22.8

(2) *T. & N. elutriator*

Material retained (%)	Test 1	Test 2
Crude	1.6	2.4
Partly opened	10.4	11.2
Open	72.0	71.2
Through 200 mesh (by difference)	16.0	15.2

(3) *Dyckerhoff air permeability test*

Surface area: 1128 $m^2\ kg^{-1}$

3.2. Specimen geometries and test procedure

Rectangular strips measuring 6 mm were used for tensile strength and three-point bending flexural strength tests conducted in a Hounsfield Tensometer and an Instron testing machine. The Young's modulus in tension (E_t) was measured using an Instron extensometer and that in bending (E_b) was calculated from the slope of the load–deflection curve taking into consideration the compliance of the testing machine.

Both three-point bend edge-notched (Fig. 1) and grooved double-cantilever-beam (DCB) (Fig. 2) specimens were used for fracture toughness testing. Equations 6 and 7 show how R_i and R are determined from the three-point bend notched beam test results using the work of fracture method. The critical stress intensity factor (K_c) is given by either (see Fig. 1)

$$K_c = \frac{1.5 P_i L a^{1/2}}{B W^2} \times [1.93 - 3.07(a/W) + 14.53(a/W)^2 - 25.11(a/W)^3 + 25.8(a/W)^4] \quad (13)$$

following Brown and Srawley [24] or by

$$K_c = \frac{1.5 P_i L}{B(W-a)^{3/2}} [Y(a/W)]^{1/2} \quad (14)$$

*The specimens prepared from these castings are thus different from the normal commercially manufactured products which have a laminated structure. Mechanical properties determined for these asbestos cements are, therefore, not necessarily representative of commercial products.

TABLE II Composition of asbestos cement

Formulation no.	Raw materials (wt %)			Composite density ρ_c (kg m^{-3})	Fibre volume fraction (v_f)
	Cassiar AK asbestos (m_f) X 10^2	Cement	Ground silica		
1	5	57	38	1550	0.030
2	10	44	36	1420	0.056
3	15	51	34	1390	0.082
4	20	48	32	1350	0.106

N.B. Density of Cassiar AK asbestos (ρ_f) $\simeq$ 2550 kg m^{-3} and $v_f = m_f(\rho_c/\rho_f)$.

after Winne and Wundt [25], where Y is a geometric correction factor and P_i is the load at crack initiation.* The difference between these two K-expressions is no more than 8% for $a/W \leqslant 0.6$ and only Equation 13 is used here to calculate K_c for the present three-point bend notched specimens.

For the DCB specimens the specific work of fracture (R) was determined using Gurney's graphical irreversible work area method as briefly outlined in Fig. 2. K_c may also be determined for this testpiece geometry if the fracture initiation load (P_i) and the instantaneous crack length (a_i) can be simultaneously recorded. Thus,

$$K_c = \frac{3.46P_i(a_i/H + 0.7)}{\sqrt{(BB_nH)}} \quad (15)$$

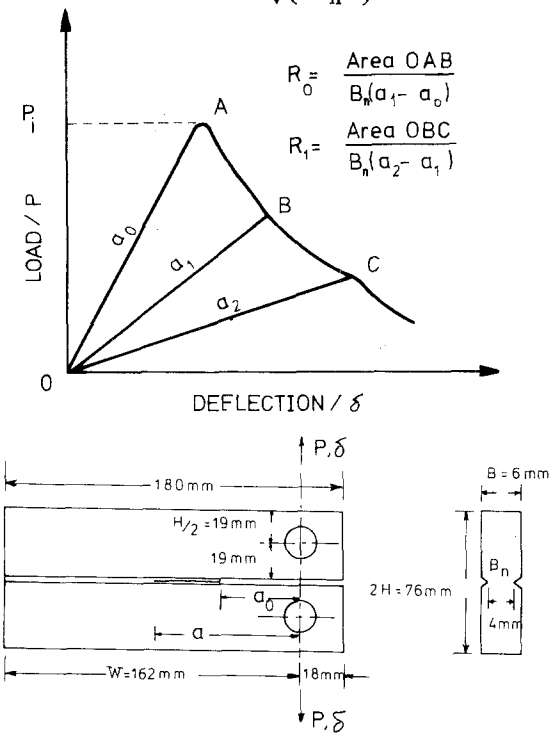

Figure 2 Illustration of the quasi-static crack propagation technique to determine R.

where B_n is the net section thickness and H is the height of one cantilever beam.

4. Results and discussion

4.1. Strength results

The ultimate tensile strength (σ_t) and the modulus of rupture (σ_b) results are shown in Figs. 3 and 4 respectively. Both σ_b and σ_t increase with increasing mass fraction of asbestos fibres (m_f) with σ_b levelling out at $m_f = 0.15$. It should be noted that the σ_b results shown in Fig. 4 contain two sets of data, one obtained by loading in the beam thickness direction and the other in the beam width direction. The good agreement between these experimental data suggests that the distribution of fibres within the cement mortar matrix is fully random. To use Equations 3 and 4 to predict σ_t and σ_b, it is necessary to determine the corresponding values of α, β, τ and the fibre aspect ratio (l/d). By back-extrapolation to $m_f = 0$ in Figs. 3 and 4, σ_m (= 3 MPa) and σ_{mb} (= 10 MPa) can be obtained for the unreinforced cement mortar matrix. Thus $\beta (= \sigma_{mb}/\sigma_m) = 3.3$ Dividing σ_b with σ_t for all the four formulations of asbestos cements and averaging these values gives $\alpha = 2.69$. Exact values of l and d for the fibres are difficult to measure since these depend on the degree of fiberization and on the milling process in which the fibres are separated into different grades by length classifiers (see Table I). Moreover, the fibres are usually bundled together (Figs. 5a and b) and they may spread open after being pulled out from the matrix (Fig. 5c). Since it is the fibre bundles that provide the reinforcement for the cement matrix, l and d measurements must therefore correspond to the fibre bundles and not the individual fibres. Both $\bar{l}$ and d were measured directly from SEM pictures taken on fracture surfaces of broken specimens. Thus the average fibre-bundle diameter (d) is approximately 25 μm and the average pull-out fibre length ($\bar{l}$) is 1 mm so that l (= $4\bar{l}$) is

*In the present experiments P_i corresponds to the maximum load.

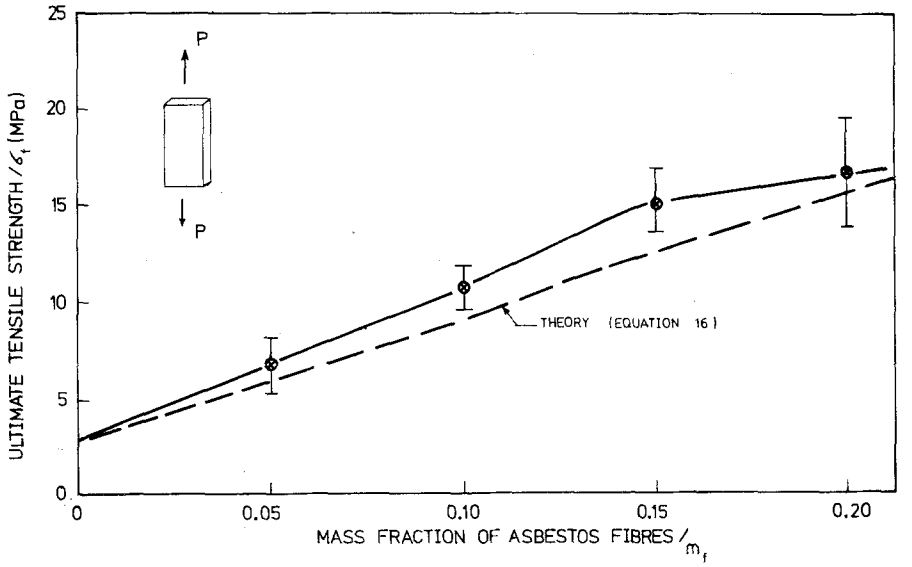

Figure 3 Variation of ultimate tensile strength with mass fraction of asbestos. Bars indicate 1 standard deviation and sample size = 10.

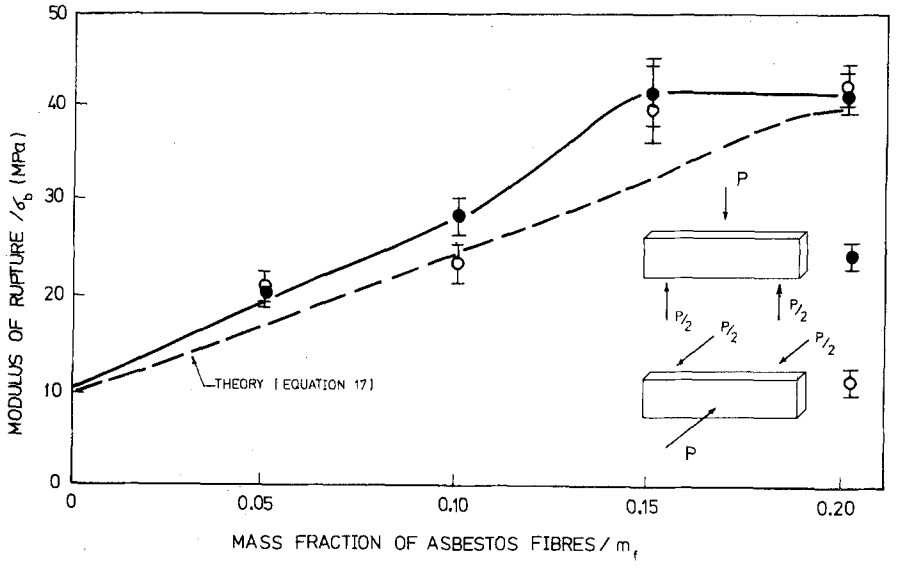

Figure 4 Variation of modulus of rupture with mass fraction of asbestos. Bars indicate 1 standard deviation and sample size = 10.

4 mm. The pull-out stress (τ) for Chrysotile fibres in a cement matrix as quoted by de Vekey and Majumdar [26] is 0.83 MPa. Using these values of l, d and τ in conjunction with Equation 1, the critical transfer length (l_c) for the fibres becomes 45 mm, assuming $\sigma_f = 3$ GPa. Therefore, the assumption of fibre pull-out in deriving the strength and toughness equations in Section 2 is justified since $l_c > l$ as calculated above. The ultimate tensile strength and the modulus of rupture equations can now be rewritten as:

$$\sigma_t = 3v_m + 108.9v_f \quad \text{(MPa)} \qquad (16)$$

and

$$\sigma_b = 8.2v_m + 292.9v_f \quad \text{(MPa)} \qquad (17)$$

where the relationship between v_f and m_f and their corresponding values are given in Table II. As shown in Figs. 3 and 4 the dashed lines predicted by Equations 16 and 17 are in reasonable agreement with experimental results. This is considered satisfactory since the maximum error is only about 18%. In fact, much better agreement between

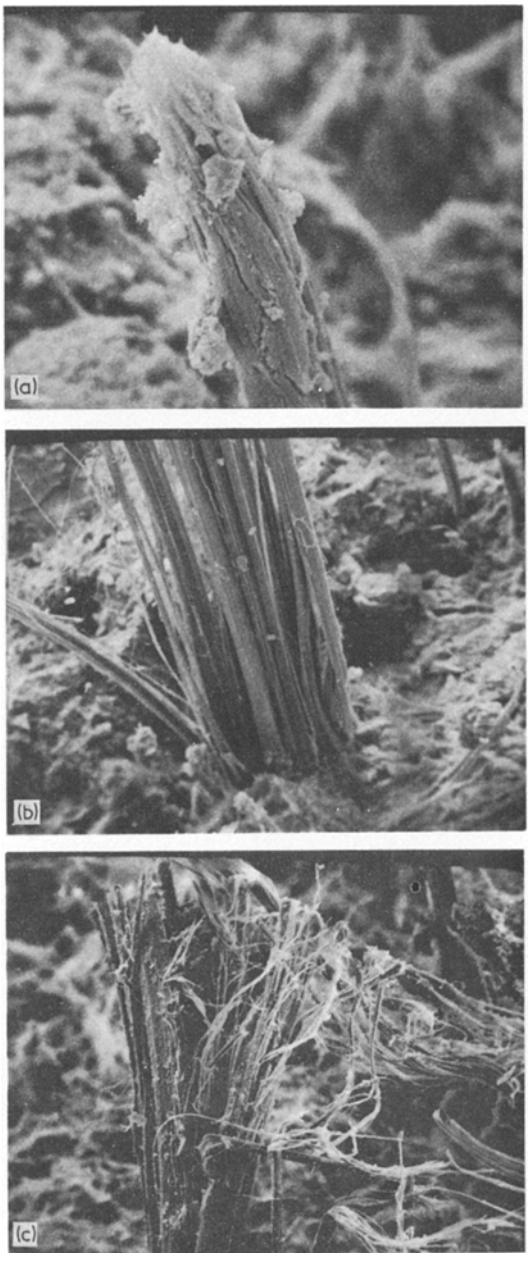

Figure 5 (a) A fibre bundle after pull-out showing cement mortar debris on fibre (× 1200). (b) A fibre bundle showing base near cement mortar matrix (× 700). (c) Opening of individual fibres of a bundle after pull-out (× 250).

theory and experiment is obtained if $\tau = 1$ MPa is used in the calculations.

Fig. 6 shows that the average Young's moduli of the asbestos cements in bending and in direct tension are independent of the mass fraction of asbestos fibres.* This behaviour is rather different from the results obtained by Allen [9] where E_t decreases almost linearly with increasing v_f. This is probably a consequence of the fact that the asbestos cements used in [9] are manufactured differently to the composites used in this work. In particular, unlike the present asbestos cements, those used by Allen have unusually large matrix void contents (v_o) which are found to increase significantly from 14% to 60% when v_f is increased from 4% to 15%. Thus his E_t values must decrease with v_f because the increase in stiffness by addition of fibres is more than offset by the reduction of the matrix stiffness due to these sharply increasing matrix voids [9]. The present results show that E_t is approximately twice E_b, an observation which has also been recently reported for Kevlar cement composites cured by autoclaving [4].

4.2. Fracture toughness results

4.2.1. Three-point bend edge-notched beam results

Fig. 7 shows a set of typical load–deflection curves for the notched beams under three-point bending. For shallow notch depths cracking was unstable. However, crack stability was improved as the notch depth was increased. It is possible to calculate K_c, R_i and R using these graphical records and Equations 13, 7 and 6, respectively. Figs. 8 to 10 show the variation of K_c, R_i and R with (a/W) for the four asbestos cement composites. As expected all these fracture parameters increase with increasing volume fraction of asbestos fibres (see Fig. 11). There is apparently no improvement in R_i and R beyond $m_f = 0.15$. The exact reason for this behaviour is presently unknown. There is not much difference in appearance of the fracture surfaces for $m_f = 0.15$ and 0.20, except perhaps for the latter there seems to be slightly more voids in the matrix. It is possible that, as a result of this, the toughness contribution by the creation of new surfaces will be reduced and the effective interfacial bond strength diminished if such voids are located close to the fibres. Also for these large fibre volume fraction composites interactions between fibres will tend to decrease the efficiency of reinforcement. All these factors added together

*Because of the small E_f/E_m and the large l/d ratios, E_t, as calculated from the rule of mixtures modified for random oriented short fibres, is essentially constant over the whole range of v_f studied. Thus E_t is approximately 19 GPa, since $E_f = 70$ GPa and $E_m = 20$ GPa.

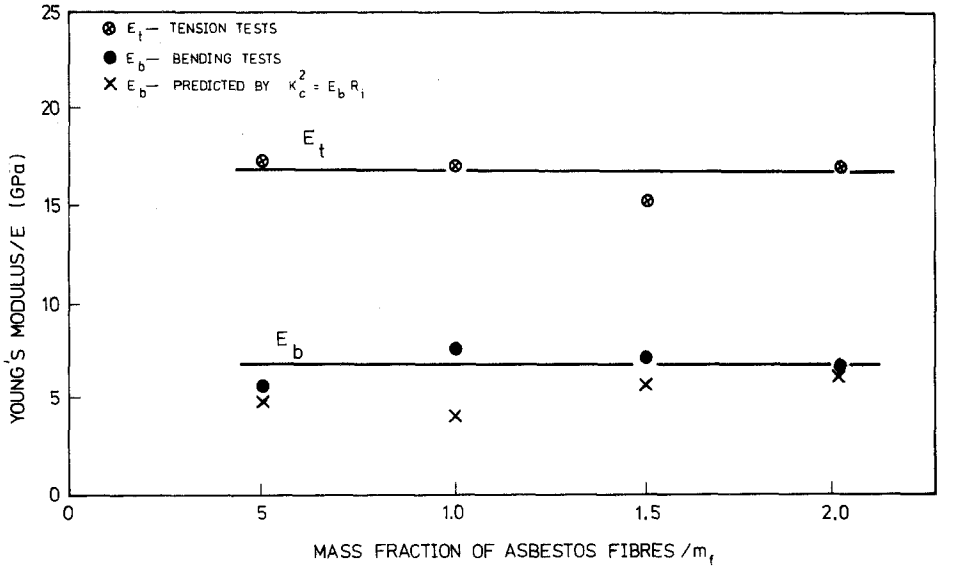

Figure 6 Variation of Young's modulus in bending and in direct tension with mass fraction of asbestos fibres.

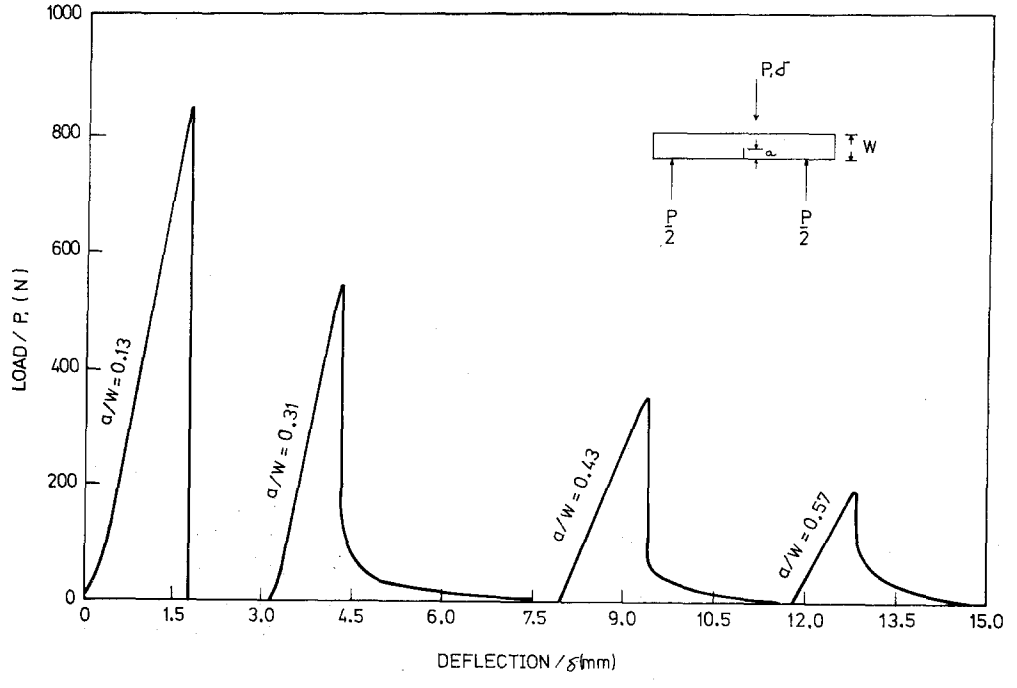

Figure 7 Load/deflection curves for asbestos cement composites with $m_f = 0.15$ and different notch depth ratios (a/W).

may have offset the predicted increase in toughness (i.e. Equation 12) with v_f beyond 15% mass fraction of fibres. It is obvious that much more serious work is needed to show exactly why additions of fibres beyond $m_f = 0.15$ does not bring about further increases in strength and toughness. In broad terms both K_c and R_i are independent of a/W. By equating $K_c^2 = E_b R_i$, E_b can be predicted using these two fracture mechanics parameters. These results are superimposed in Fig. 6 and they agree reasonably well with corresponding measured E_b values. The specific work of fracture (R) (including the crack initiation and propagation energies), however, decreases with

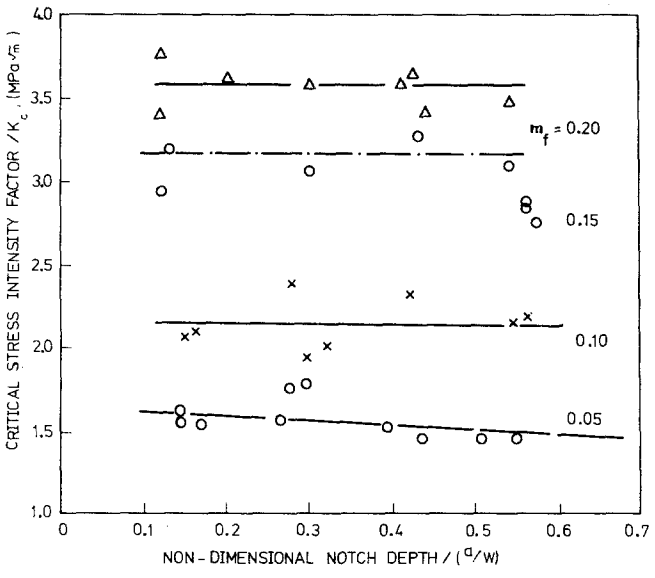

Figure 8 Variation of K_c with notch depth ratio (a/W) for asbestos cements with different fibre mass fractions (three-point bend edge notched specimens).

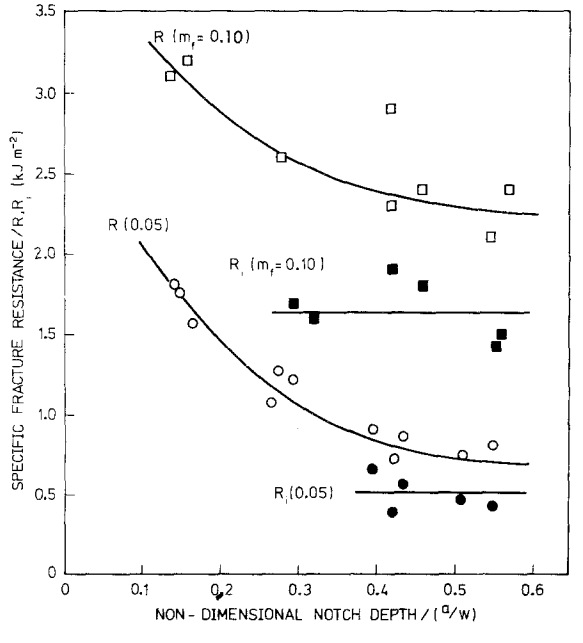

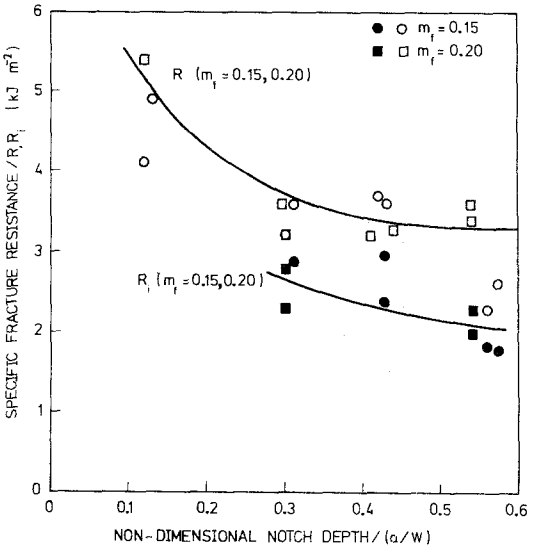

Figures 9 and 10 Variation of specific work of fracture (R) and specific crack initiation energy (R_i) with notch depth ratio (a/W) for asbestos cements with different mass fractions of fibres (three-point bend edge-notched specimens).

a/W and tends to level out at $a/W \geqslant 0.4$. It should be noted that R has obviously been over-estimated at small a/W where cracking is unstable.

J_c for the asbestos cements were calculated using the following equation [27]:

$$J_c = \frac{2}{B(W-a)} \int_0^{\delta_{crack}} P d\delta_{crack} \qquad (18)$$

i.e.
$$J_c = \frac{2}{B(W-a)} (U_i - U_0) \qquad (18a)$$

where U_i and U_0 are respective areas under the P–δ curves for the notched and unnotched beams integrated to the fracture-initiation load of the notched beam. Table III shows that J_c agrees fairly well with R_i for all the asbestos cements.

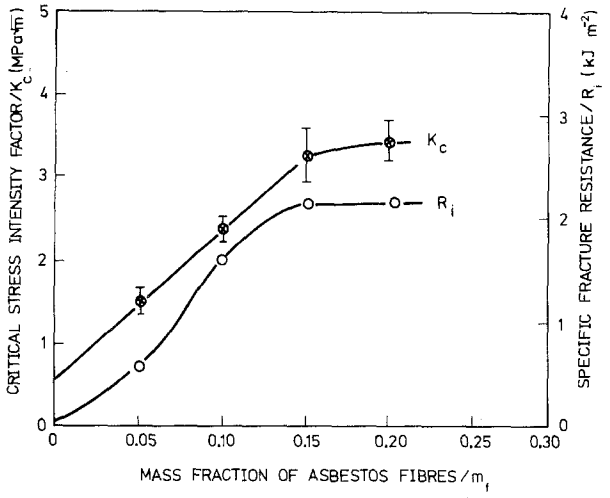

Figure 11 Variation of K_c and R_i with mass fraction of asbestos fibres. Bars indicate 1 standard deviation.

TABLE III J_c and R_i results for asbestos cements using three-point bend notched beams

Sample	m_f	a/W	J_c (kJ m^{-2})	R_i (kJ m^{-2})
1–7e	0.05	0.51	0.34	0.43
1–7f	0.05	0.55	0.35	0.47
2–7e	0.10	0.55	1.51	1.43
2–7f	0.10	0.56	1.50	1.50
3–7d	0.15	0.56	1.23	1.70
3–7e	0.15	0.57	1.80	1.80
4–7e	0.20	0.54	1.58	2.00
4–7f	0.20	0.54	1.95	2.20

4.2.2. Double-cantilever-beam specimen results

Fig. 12 shows a typical load–deflection curve for quasi-static cracking in a grooved DCB specimen. Cracking was in general stable, as would be anticipated for this specimen geometry made from a material with constant R [28]. However, there were a few cases where the grooves were not deep enough to constrain the crack from veering out of the arms. Figs. 13 and 14 show the variation of R as the crack length increases. Only those data obtained from specimens with a straight crack are included in these plots. The increase of R with increasing a/W may be simply explained by the fact that fibres bridging the gap and behind the crack front are also pulled-out as the crack advances. The starting a/W for these DCB specimens were approximately 0.30, and at this initial crack length the R values for the different asbestos cements were close to the corresponding R_i values obtained from three-point bend notched specimens. It should also be pointed out that the upper and

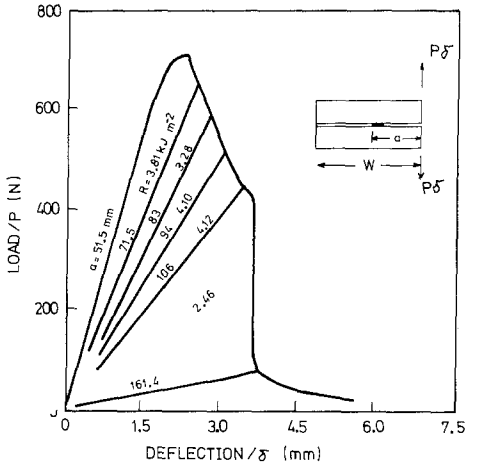

Figure 12 Load–deflection curve for quasi-static crack propagation in a DCB specimen with $m_f = 0.20$ and $B_n = 4.02$ mm.

lower bound R values derived from these two specimen geometries are consistent although the trends of R varying with a/W are exactly opposite. The decreasing trend of R with a/W for the three-point bend notched specimens is thought to be associated with increasing control of crack growth and hence decreasing kinetic energy losses as the notch depth increases [29]. In the DCB specimens cracking is quasi-static so that kinetic energy losses are negligible.

Equation 15 has also been used to calculate K_c for the DCB specimens. As shown in Table IV these K_c results agree very well with corresponding values derived from three-point bend notched beams. This indicates that K_c is a usable material parameter for the asbestos-cement composites.*

*Recent experimental K_c results obtained from large single-edge-notched (SEN) specimens [30] compare favourably with corresponding values derived from these DCB and three-point bend notched specimens.

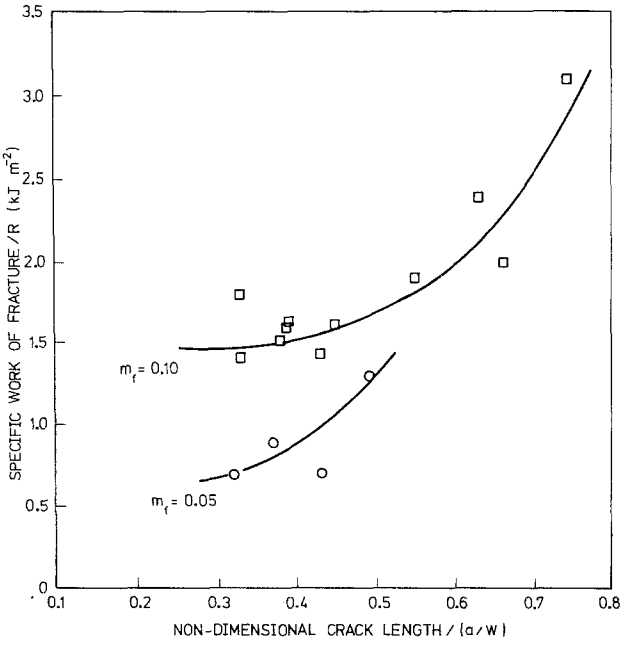

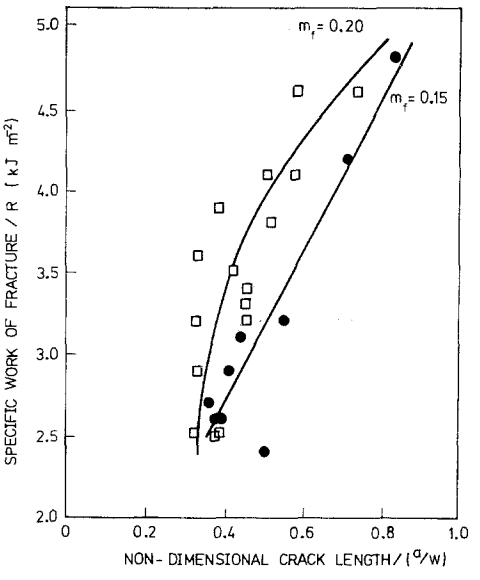

Figures 13 and 14 Variation of R with non-dimensional crack length (a/W) for different asbestos cements (DCB specimens).

TABLE IV Comparison of K_c in DCB specimens and three-point bend notched beams

Asbestos content	DCB specimens		Three-point bend notched beams	
(m_f)	K_c (MPa$\sqrt{m}$)	Sample size	K_c (MPa$\sqrt{m}$)	Sample size
0.05	1.74 ± 0.31*	5	1.53 ± 0.17*	11
0.10	2.52 ± 0.27	9	2.34 ± 0.18	8
0.15	3.38 ± 0.34	8	3.25 ± 0.38	8
0.20	3.66 ± 0.24	9	3.44 ± 0.29	8

*1 standard deviation.

4.2.3. Prediction of fracture toughness of asbestos cements

Fig. 15 shows a typical fracture surface of the asbestos cements where the fibre pull-out mechanism is clearly displayed. R_s and R_{po} have been calculated using Equations 11 and 9 and the following values: $l = 4$ mm, $d = 25\ \mu$m, $\tau = 0.83$ MPa and $R_m = R_{if} = 20$ J m^{-2} (by back-extrapolation of the R_i curve in Fig. 11 to $m_f = 0$). Table V shows that the predicted R-values ($= R_s + R_{po}$) are in reasonably good agreement with corresponding experimental fracture toughness results obtained from DCB specimens. Since $R_{po} \gg R_s$ the source of fracture toughness of asbestos cement mortar composites is predominantly due to the fibre pull-out process. The energies absorbed in creating new surfaces – matrix and interface debonding – contribute only approximately 5% of the total specific fracture work.

Figure 15 A typical SEM fracture surface of an asbestos cement ($m_f = 0.15$) showing the predominant fibre pull-out mechanism (× 35).

TABLE V Prediction of fracture toughness in asbestos cements.

m_f	v_f	R_s (kJ m^{-2})	R_{po}(kJ m^{-2})	$R_s + R_{po}$(kJ m^{-2})	R(kJ m^{-2})
0.05	0.030	0.06	1.09	1.15	0.92 ± 0.28*($n^{\dagger} = 10$)
0.10	0.56	0.09	2.03	2.12	1.60 ± 0.60 ($n = 18$)
0.15	0.082	0.12	2.98	3.10	2.92 ± 0.68 ($n = 24$)
0.20	0.106	0.15	3.85	4.00	3.37 ± 0.80 ($n = 24$)

$^{\dagger}n$ = sample size of experimental data obtained in DCB specimens.
*1 standard deviation.

5. Conclusions

The strength and fracture properties of asbestos cement mortar composites with m_f between 0.05 to 0.20 have been studied in this paper. It is found that the modified law of mixtures strength Equations 3 and 4 give fairly good agreement in σ_t and σ_b with experimental results. The critical stress intensity factor (K_c) and the specific crack-initiation energy (R_i) measured from DCB specimens and three-point bend edge-notched testpieces are consistent with one another and may therefore be regarded as usable material properties. The specific work of fracture (including both initiation and propagation energies) (R) is shown to increase with increasing crack length in DCB specimens, owing to fibres bridging the crack tips. R-values for the asbestos cement composites can be reasonably well predicted by considering the energies absorbed in both the fibre pull-out and the fibre–matrix interface debonding processes. The fibre pull-out mechanism contributes more than 95% of the total fracture work and is thus the major source of fracture toughness in the asbestos cements.

Acknowledgements

This work is financially supported by a research grant from James Hardie and Coy Pty Ltd, Australia. The author wishes to thank Dr A. Abel for placing the testing facilities of the Materials/Structures Laboratory of Civil Engineering Department at his disposal. Thanks are also due to Drs A. G. Atkins and R. N. Swamy for critical comments of an earlier version of the manuscript.

References

1. A. J. MAJUMDAR, J. M. WEST and L. J. LARNER, *J. Mater. Sci.* **12** (1977) 927.
2. P. L. WALTON and A. J. MAJUMDAR, *Composites* **6** (1975) 209.
3. M. A. ALI, A. J. MAJUMDAR and B. SINGH, *J. Mater. Sci.* **10** (1975) 1732.
4. P. L. WALTON and A. J. MAJUMDAR, *ibid* **13** (1978) 1075.
5. J. AVESTON, *ibid* **4** (1969) 625.
6. C. J. MARTIN and V. A. PHILLIPS, *Mat. Sci. Eng.* **30** (1977) 81.
7. D. WALSH, M. A. OTOONI, M. E. TAYLOR Jr and M. J. MARCINKOWSKI, *J. Mater. Sci.* **9** (1974) 423.
8. J. D. BIRCHALL, A. J. HOWARD and J. E. BAILEY, *Proc. Roy. Soc. London* **A360** (1978) 445.
9. H. G. ALLEN, *Composites* **2** (1971) 98.
10. J. P. ROMUALDI and J. A. MANDEL, *J. Amer. Concr. Inst.* **61** (1964) 657.
11. R. N. SWAMY and P. S. MANGAT, *Proc. Inst. Civil Eng.* **57** (1974) 701.
12. M. F. KAPLAN, *J. Amer. Concr. Inst.* **58** (1961) 591.
13. J. H. BROWN, *Mag. Concr. Res.* **24** (1972) 185.
14. B. HARRIS, J. VARLOW and C. D. ELLIS, *Cem. Concr. Res.* **2** (1972) 447.
15. S. MINDESS and J. S. NADEAU, *ibid* **6** (1976) 529.
16. F. RADJY and T. C. HANSEN, *ibid* **3** (1973) 343.
17. S. MINDESS, F. V. LAWRENCE and C. E. KESLER, *ibid* **7** (1977) 731.
18. J. R. RICE, *J. Appl. Mech. Trans. ASME* **35** (1968) 379.
19. H. G. TATTERSALL and G. TAPPIN, *J. Mater. Sci.* **1** (1966) 296.
20. S. K. GAGGAR and L. J. BROUTMAN, *Fibre Sci. Technol.* **9** (1976) 205.
21. C. GURNEY and J. HUNT, *Proc. Roy. Soc. London* **A299** (1967) 508.
22. W. A. PATTERSON and H. C. CHAN, *Composites* **6** 1975) 102.
23. T. U. MARSTON, A. G. ATKINS and D. K. FELBECK, *J. Mater. Sci.* **9** (1974) 447.
24. W. F. BROWN Jr and J. E. SRAWLEY, STP410, American Society for Testing and Materials (1966).
25. D. H. WINNE and B. M. WUNDT, *Trans. ASME* **80** (1958) 1643.
26. R. C. DE VEKEY and A. J. MAJUMDAR, *Mag. Concr. Res.* **20** (1968) 229.
27. J. R. RICE, P. C. PARIS and J. G. MERKLE, STP 536, American Society for Testing and Materials (1973) pp. 231–45.
28. C. GURNEY and Y. W. MAI, *Eng. Fract. Mech.* **4** (1972) 853.
29. R. W. DAVIDGE and G. TAPPIN, *J. Mater. Sci.* **3** (1968) 165.
30. Y. W. MAI, unpublished research, Sydney University (1978).

Received 27 September and accepted 18 December 1978.